

# Selective oxidation of carbolide C–H bonds by an engineered macrolide P450 mono-oxygenase

Shengying Li<sup>a</sup>, Mani Raj Chaulagain<sup>b</sup>, Allison R. Knauff<sup>b</sup>, Larissa M. Podust<sup>c</sup>, John Montgomery<sup>b,1</sup>, and David H. Sherman<sup>a,b,d,1</sup>

<sup>a</sup>Life Sciences Institute and Department of Medicinal Chemistry, <sup>b</sup>Department of Chemistry, and <sup>d</sup>Department of Microbiology and Immunology, University of Michigan, Ann Arbor, MI 48109; and <sup>c</sup>Department of Pharmaceutical Chemistry, University of California, San Francisco, CA 94158

Edited by Christopher T. Walsh, Harvard Medical School, Boston, Massachusetts, and approved September 3, 2009 (received for review June 27, 2009)

**Regio- and stereoselective oxidation of an unactivated C–H bond remains a central challenge in organic chemistry. Considerable effort has been devoted to identifying transition metal complexes, biological catalysts, or simplified mimics, but limited success has been achieved. Cytochrome P450 mono-oxygenases are involved in diverse types of regio- and stereoselective oxidations, and represent a promising biocatalyst to address this challenge. The application of this class of enzymes is particularly significant if their substrate spectra can be broadened, selectivity controlled, and reactions catalyzed in the absence of expensive heterologous redox partners. In this study, we engineered a macrolide biosynthetic P450 mono-oxygenase PikC (PikC<sub>D50N</sub>-RhFRED) with remarkable substrate flexibility, significantly increased activity compared to wild-type enzyme, and self-sufficiency. By harnessing its unique desosamine-anchoring functionality via a heretofore under-explored “substrate engineering” strategy, we demonstrated the ability of PikC to hydroxylate a series of carbocyclic rings linked to the desosamine glycoside via an acetal linkage (referred to as “carbolides”) in a regioselective manner. Complementary analysis of a number of high-resolution enzyme-substrate cocrystal structures provided significant insights into the function of the aminosugar-derived anchoring group for control of reaction site selectivity. Moreover, unexpected biological activity of a select number of these carbolide systems revealed their potential as a previously unrecorded class of antibiotics.**

cytochrome P450 mono-oxygenase | PikC | RhFRED | substrate engineering

The superfamily of cytochrome P450 enzymes (mono-oxygenases) is involved in diverse oxidative processes, including xenobiotic catabolism, steroid synthesis, and biosynthetic tailoring of diverse natural products (1–3). Among various reactions catalyzed by P450 enzymes, the regio- and stereoselective oxidation of an unactivated sp<sup>3</sup> C–H bond represents a central challenge in organic chemistry (4–8). Considerable effort has been devoted to identifying biological catalysts or simpler mimics that function by mechanisms typically involving a metal oxo-reactive site (9). Alternatively, transition metal complexes have been identified for C–H bond oxidations that proceed through mechanisms completely distinct from biological systems. A key challenge in developing useful C–H oxidation procedures is the control of site-selectivity among similar C–H bonds. Successful approaches have typically involved either relying on the inherent reactivity differences of various C–H bonds, based on steric and electronic considerations (10–15), or the incorporation of directing groups that orient the catalyst active site toward a specific C–H bond (16–18). The selective oxidation of a C–H bond that is neither inherently more reactive than alternate sites nor positioned adjacent to a directing group poses the most difficult application in site-selective C–H bond functionalization.

Recent reports have shown that supramolecular organometallic assemblies can provide some success in this challenge for synthetic chemistry (19–24). Alternatively, biological catalysts may provide unique potential to selectively oxidize bonds that are chemically similar, yet remote from directing influences. Thus, we were drawn to investigate the potential role of biosynthetic P450 mono-

oxygenases, despite their fundamental dependence on substrate-enzyme complementarity, which might limit their application in synthetic chemistry (25). A number of previous efforts have sought to overcome this limitation by employing protein engineering strategies, including scanning chimeragenesis (26, 27) and directed-evolution (28–31) to generate nonnatural cytochrome P450s (e.g., P450<sub>BM3</sub>) with desired substrate specificities and abilities to selectively oxidize target substrates.

Based on a series of investigations involving P450 mono-oxygenases with remarkable substrate flexibility in macrolide biosynthetic systems (32, 33), we were motivated to explore their potential value in selective C–H bond activation reactions (25). Their unique requirement for a sugar-appended substrate led us to assess an under-explored strategy involving “substrate engineering” (Fig. 1) that offers another way to broaden the substrate landscape of biological catalysis (34, 35). Our anchoring/tethering approach was inspired by an earlier observation that certain functional groups facilitate enzyme-substrate interactions, where a direct functional group linkage (termed “anchoring group” in this study) to previously inaccessible compounds enables selective oxidation of the modified substrates *in vivo* (36, 37). However, because of the complexity of the cell-based system, the precise mechanism behind the substrate engineering approach has remained unclear. An initial application (36) hypothesized that the anchoring group might be involved in substrate recognition, productive binding, or control of binding orientation in the active site of certain oxidative enzymes (e.g., mono-oxygenases).

Here, we report *in vitro* implementation of substrate engineering for selective C–H bond oxidations by using an optimized form of the macrolide P450 mono-oxygenase PikC (32, 38). For this study, a series of carbocyclic rings linked to the desosamine glycoside (referred to as “carbolides”) were effectively hydroxylated in a regioselective manner. Furthermore, analysis of a series of high-resolution enzyme-substrate cocrystal structures provided significant insights into the function of the aminosugar-derived anchoring group for control of reaction site selectivity. Finally, unexpected biological activity of a select number of these carbolide systems revealed their potential as an unusual class of antibiotics.

## Results and Discussion

**Engineered PikC<sub>D50N</sub>-RhFRED Is Capable of Hydroxylating Carbolides Effectively and Regioselectively.** PikC is the cytochrome P450 involved in pikromycin biosynthesis from *Streptomyces venezuelae* (32,

Author contributions: S.L., J.M., L.M.P., and D.H.S. designed research; S.L., M.R.C., A.R.K., and L.M.P. performed research; S.L., M.R.C., A.R.K., L.M.P., J.M., and D.H.S. analyzed data; and S.L., L.M.P., J.M., and D.H.S. wrote the paper.

The authors declare no conflict of interest.

This article is a PNAS Direct Submission.

Data deposition: The atomic coordinates and structure factor have been deposited in the Protein Data Bank, www.pdb.org (PDB ID codes 2W19 and 2WHW)

<sup>1</sup>To whom correspondence may be addressed. E-mail: jmontg@umich.edu or davidhs@umich.edu.

This article contains supporting information online at [www.pnas.org/cgi/content/full/0907203106/DCSupplemental](http://www.pnas.org/cgi/content/full/0907203106/DCSupplemental).

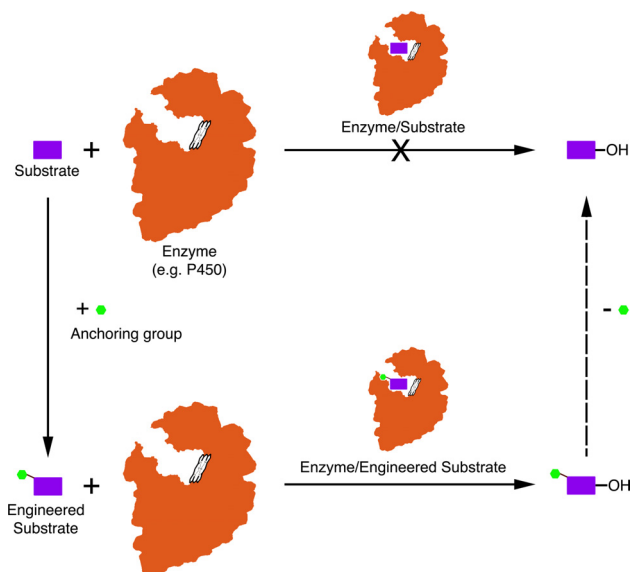


Fig. 1. Schematic strategy of substrate engineering.

39). The physiological function of this mono-oxygenase is to hydroxylate both the 12-membered ring macrolide YC-17 (structure 1) and the 14-membered ring macrolide narbomycin (structure 4), giving rise to methymycin/neomethymycin (structures 2 and 3) and pikromycin (structure 5), respectively, as major products (Fig. 2). Recent analysis of X-ray cocrystal structures of PikC (40, 41) involving endogenous substrates revealed that the macrolactone ring contacts the active site residues entirely via nonspecific hydrophobic interactions, likely accounting for the tolerance of PikC toward the variant macrolactone ring size and functionalization. In contrast, the desosamine sugar employs two distinct binding pockets and anchors the substrate through a number of hydrogen bonds and ionic interactions, in particular, a unique salt bridge between the protonated dimethylamino group of desosamine and a glutamate residue, either Glu-94 or Glu-85 in the B/C loop region. Based on these previously recognized molecular interactions that specify substrate binding affinity and orientation in the binding pocket, we reasoned that desosamine could be an effective anchoring group to direct positioning of various unnatural molecules in the active site of PikC for selective C–H bond hydroxylations.

To test this hypothesis, we synthesized the unnatural cyclic carbolide substrate desosaminyl cyclododecane (structure 6) to mimic the structure of the natural substrate YC-17 (structure 1) using a recently developed synthetic strategy (33), which was subsequently used as a general approach to derivatize diverse

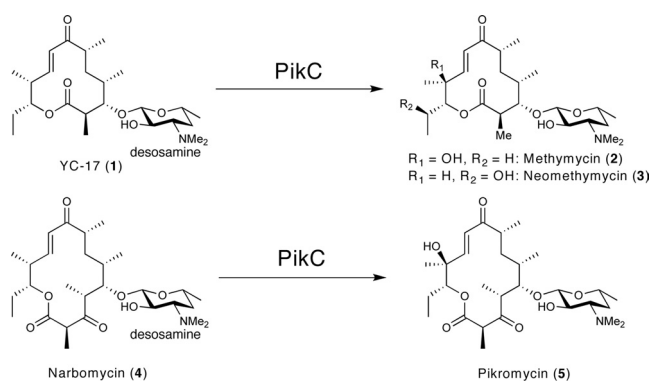


Fig. 2. Major physiological reactions catalyzed by PikC.

alcohols with desosamine (Fig. S1 in *SI Appendix*). An enzyme-substrate analysis showed that structure 6 binds to wild type PikC (PikC<sub>wt</sub>) with a dissociation constant ( $K_d$ ) of 1,379  $\mu\text{M}$ ,  $\approx 12\times$  higher than the  $K_d$  value (116  $\mu\text{M}$ ) of structure 1. The decreased binding affinity of structure 6 could result from: (i) an entropic penalty upon binding because of high conformational freedom of the saturated ring system; (ii) lack of hydrophobic interactions between the functional groups on the macrolactone ring of structure 1 and PikC active site residues; and (iii) loss of some specific interactions with desosamine, as observed in the cocrystal structure with PikC (see below). When using the more active PikC<sub>D50N</sub> mutant (40, 41), the binding affinities of both carbolide (structure 6) and macrolide (structure 1) were shown to be  $\approx 4\times$  higher, with  $K_d$  values of 390 and 32  $\mu\text{M}$ , respectively. Moreover, we recently engineered a self-sufficient fusion enzyme PikC-RhFRED (38) that displayed  $\approx 4$ -fold enhanced catalytic activity ( $k_{cat}$ ) compared to PikC<sub>wt</sub>. Combining these two beneficial properties, the resulting engineered form of the P450 enzyme PikC<sub>D50N</sub>-RhFRED ( $k_{cat}/K_m = 7.44 \mu\text{M}^{-1}\text{min}^{-1}$  for structure 1) (Fig. S2 in *SI Appendix*) is  $\approx 13\times$  more active than PikC<sub>wt</sub> (38). Interestingly, structure 1 and structure 6 bound to this mutant enzyme with slightly improved  $K_d$  values of 19 and 309  $\mu\text{M}$  (Table 1), respectively. Because of enhanced substrate conversion and ease of use in the absence of expensive exogenous redox partners, we elected to employ PikC<sub>D50N</sub>-RhFRED to hydroxylate carbolide (structure 6) and all other substrates for this work.

Liquid chromatography-mass spectrometry (LC-MS) analysis (Fig. 3A) of the extract obtained following reaction with PikC<sub>D50N</sub>-RhFRED showed that 47% of carbolide (structure 6) was converted into seven different monohydroxylated products (structures 7a–7g) (no multihydroxylated products were observed) with expected  $m/z = 358.19$  for structure 6 + OH + H<sup>+</sup> using 5  $\mu\text{M}$  PikC<sub>D50N</sub>-RhFRED in 3 h (the conversion can be driven further by increasing enzyme concentration or reaction time). All product ions displayed the same MS/MS spectra (Fig. S3 in *SI Appendix*) at  $m/z = 158.02$ , corresponding to desosamine–OH<sup>+</sup>. The unmodified desosamine moiety indicates that all hydroxylations occur on the cyclododecane ring. In contrast, cyclododecanol lacking an appended desosamine was unable to serve as a substrate for PikC P450 under identical conditions. Therefore, it is evident that desosamine is indispensable for this biochemical transformation. Notably, PikC<sub>wt</sub>, PikC<sub>D50N</sub>, and PikC<sub>wt</sub>-RhFRED generated similar product profiles compared to PikC<sub>D50N</sub>-RhFRED, albeit with lower efficiency. These results indicate that neither the point mutation nor the C-terminal RhFRED-fusion with PikC has a significant impact on the binding mode of structure 6.

To assess the regio- and stereoselectivity of PikC<sub>D50N</sub>-RhFRED toward the selected substrate, we sought to obtain detailed structural information on the reaction products. Challenging preparative-scale separations, as well as the high similarity of the methylene groups on the cyclododecane ring, complicated structure determination of the individual compounds by NMR analysis. Because of the large number of potential isomers (23 total) that could result from oxidation of the 12-membered ring of structure 6, it was impractical to synthesize all possible products. Therefore, guided by the 2.0-Å cocrystal structure of mutant PikC<sub>D50N</sub> enzyme with structure 6 (Fig. 4), we synthesized a series of authentic standards with a hydroxyl group installed at the C7 and C6/C8 position (the two diastereotopic carbons were numbered differently for clarity) that were likely to be the major reaction products. During the chemical synthesis, but before desosamine installation, racemic mixtures of two diastereomers of a monoprotected diol leading to C6/C8-oxidized authentic materials were prepared. Glycosylation, with the glycosyl fluoride of acetate-protected desosamine followed by deprotection, provided the four diastereomers that correspond to C6/C8 oxidized products (see *SI Appendix*). Similarly, the two diastereomers of C7-oxidized authentic material were obtained.

Through comparison of LC-MS retention times and confirma-



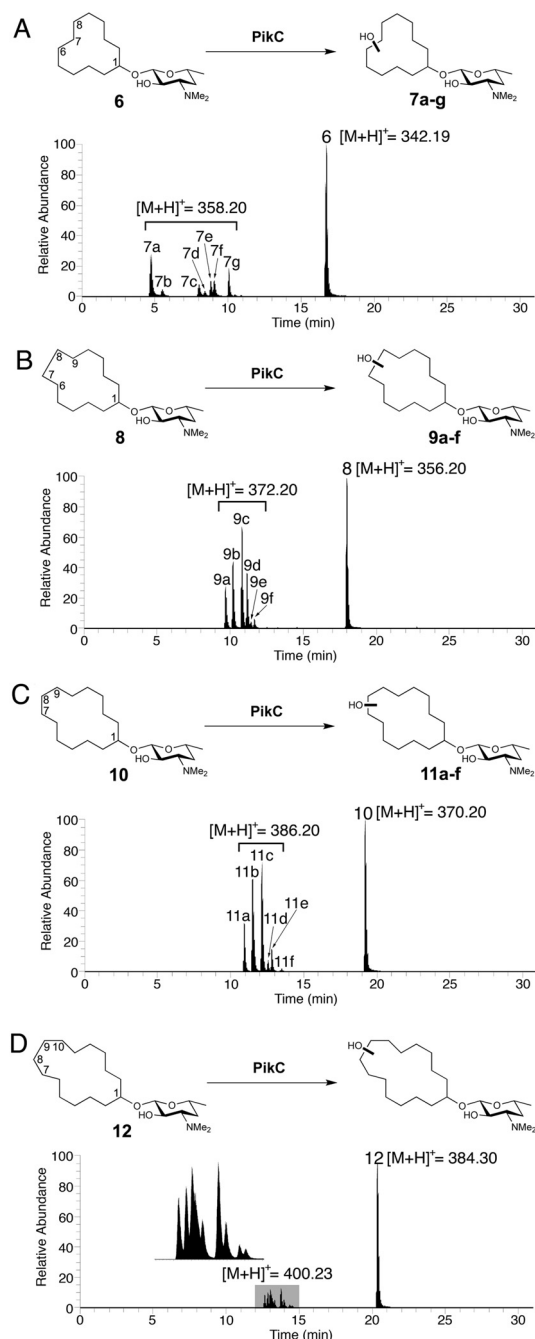


**Fig. 3.** LC-MS analysis of  $\text{PikC}_{\text{D50N}}$ -RhFRED catalyzed reactions using different cyclized carbolides as substrates. (Ion count chromatograms are shown.) (A) Desaminyl cyclododecane (structure **6**) reaction; structures **7b** and **7f** correspond to two diastereomers generated by C7 hydroxylation; structures **7a**, **7c**, **7e**, and **7g** correspond to four diastereomers generated by C6/C8 hydroxylation. (B) Desaminyl cyclotridecane (structure **8**) reaction; structures **9a**, **9d**, and **9f** correspond to diastereomers arising from C6/C9 hydroxylation; structures **9b** and **9c** correspond to diastereomers originated from C7/C8 or C6/C9 hydroxylation. The number of products that peak **9c** contains is undetermined because of product overlap. (C) Desaminyl cyclotetradecane (structure **10**) reaction. (D) Desaminyl cyclopentadecane (structure **12**) reaction. The details of product assignment for structures **6** and **8** based on correlation with synthesized authentic standards regarding retention time and coinjection confirmation are shown in the *SI Appendix*.

(Table S2 in *SI Appendix*, and see Figs. 4 and 5) of  $\text{PikC}_{\text{D50N}}$  in complex with unnatural substrates (structures **6** and **8**).

In the cocrystal structure of  $\text{PikC}_{\text{D50N}}$  and structure **6**, the

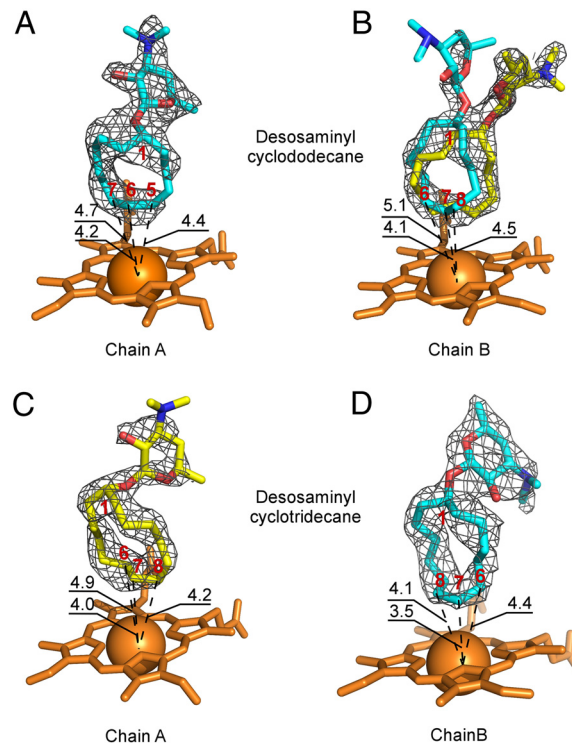


**Fig. 4.** Multiple binding modes of desaminyl cycloalkanes. Orientations of structure **6** in the active site of  $\text{PikC}_{\text{D50N}}$  (A) in chain A and (B) in chain B, and orientations of structure **8** in the active site of  $\text{PikC}_{\text{D50N}}$  (C) in chain A and (D) in chain B, as defined by the fragments of the electron density map (gray mesh) contoured at  $0.8\sigma$  are shown. In (B), structure **6** is docked in the flipped-over orientations, allowing hydroxylation on the both sides of the ring. In (C) and (D), structure **8** is in flipped-over orientations. Heme is shown in orange. Oxygen atoms are in red, nitrogen in blue, iron in orange (shown as a Van der Waals sphere). Atoms of the cycloalkane ring are labeled in red. Distances are in Angstroms. Images are generated using PYMOL.

electron density for structure **6** is well defined in one monomer of the asymmetric unit (see Fig. 4A). In contrast, the other monomer showed an unambiguously positioned cyclododecane ring, while the dispersed electron density for desosamine indicated at least two alternative conformations (see Fig. 4B). A satisfactory fit was achieved when structure **6** was docked in two flipped orientations. The carbolide (structure **6**) binds in the active site in the L-shaped conformation bringing four cyclododecane carbons most remote from the desosamine anchoring group within  $5 \text{ \AA}$  of the Fe reaction center (see Fig. 4A and B), revealing that C5, C6, C7, and C8 are the likely hydroxylation sites. The observed pattern of regioselectivity could arise from sporadic contacts of the desosamine moiety of structure **6** with a number of amino acid residues (see Fig. 5A). Indeed, the specific salt-bridge involving E94 is found in only one conformer (pink in Fig. 5A) of structure **6**, and a number of the chain A active-site residues (green) (including F178, I239, V242, and M394) adopt alternative conformations indicative of dynamic interactions with the substrate. In chain B, although the salt-bridge to E94 is lost, E246 (ice blue in Fig. 5A) is located within electrostatic distance from the dimethylamino group of the proximal conformer (cyan). However, the E246 side chain is missing from the electron-density map of chain A. In addition, the suboptimal regioselectivity could be caused by the inherent flexibility of the large cycloalkane ring. Because all six diastereomers arising from the C7 and C6/C8 hydroxylated regioisomers were observed, there is clearly a lack of stereoselectivity from this enzymatic transformation. The cocrystal structure suggests that compromised stereoselectivity is likely caused by flipping (or rotating) of the carbolide

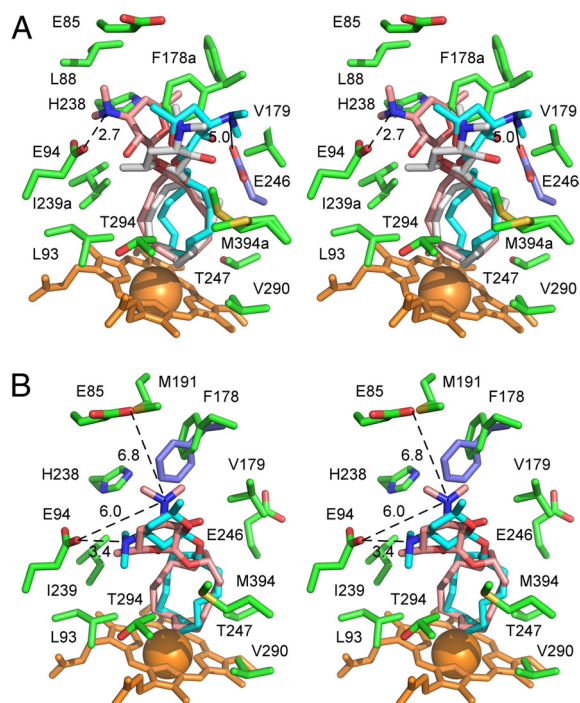


**Fig. 5.** Desosaminyl cycloalkane binding sites. (A) Stereoview of the  $\text{PikC}_{\text{D50N}}$  binding site with the three superimposed structure **6** conformers highlighted (gray) in chain A and (pink and cyan) chain B, surrounded by the chain-A amino acid side chains within 5 Å plus E85 (green). E246 of chain B is highlighted in ice blue. For clarity, V242 was omitted from the drawing. (B) Stereoview of the  $\text{PikC}_{\text{D50N}}$  binding site with two superimposed structure **8** conformers highlighted (pink) in chain A and (cyan) chain B, surrounded by the chain A amino acid side chains within 5 Å plus E85. F178 of chain B is highlighted in ice blue. Heme is shown in orange. Oxygen atoms are in red, nitrogen in blue, iron in orange (shown as a Van der Waals sphere). Distances between tertiary amine and carboxylic groups are in Angstroms. Lowercase “a” in the residue label indicates that alternative conformations are shown.

substrate in the  $\text{PikC}$  active site, resulting in oxidation on both faces of the ring (see Fig. 4 *A* and *B*).

Further inspection of the cocrystal structures revealed that, whereas three orientations are distinguishable for structure **6**, only two orientations (one in each protein monomer in the asymmetric unit) are observed for structure **8** in the 2.2-Å X-ray cocrystal structure (see Figs. 4 and 5), suggesting improved complementarity or more limited conformational freedom of the larger ring in the active site. This could explain the increased binding affinity ( $K_d = 218 \mu\text{M}$ ) and hence reactivity (65% yield) of structure **8** compared to structure **6** ( $K_d = 309 \mu\text{M}$ , 47% yield). In one monomer (cyan in Fig. 5*B*), the desosamine moiety is in salt-bridge contact with E94, while in the other monomer (pink) it is within electrostatic distance from both E94 and E85. Amino acid side chains in the active site are stabilized in a single conformation, with the exception of F178, which is represented by different conformers in chain A (green) and chain B (ice blue) (see Fig. 5*B*). Similar to structure **6**, the cocrystal structure suggests that flipping-over (or rotation) of structure **8** in the active site could enable hydroxylation (likely at C6/C9 or C7/C8) on both faces of the ring. However, a more limited resolution of the product profile in the LC-MS analysis (see Fig. S6 in *SI Appendix*) (unlike oxidations of compound structure **6**, where oxidation products were better distinguished by LC-MS) (see Fig. S4 in *SI Appendix*) prevents verification of this prediction, or further evaluation of the reaction stereoselectivity.

Despite previously demonstrated dynamics of  $\text{PikC}$  (40), no induced-fit conformational changes were observed in response to binding of the various carbolides, which could potentially

prevent the substrate from wobbling in the active site. This observation contradicts the concept of “conformational plasticity” applied for mammalian P450 enzymes (42), and limits the role of  $\text{PikC}$  conformational dynamics to substrate access to and product release from the active site.

**Antibacterial Activities of Synthetic Desosaminyl Derivatives.** In macrolide antibiotics, desosamine (or a related deoxysugar moiety) has been found to play a crucial role in the interaction of these important compounds with the 23S ribosomal RNA (the major drug target for macrolides) through a number of specific contacts with ribonucleotides in the peptidyl-transferase center (43). Accordingly, we surmised that our series of synthetic desosaminyl derivatives might possess antibacterial activity. As shown in Table S3 in *SI Appendix*, the cyclic carbolides including structures **6**, **8**, **10**, and **12** displayed some inhibitory activities against selected microbial targets, while their corresponding aglycones were inactive, confirming the significance of desosamine for bioactivity. Remarkably, the aromatic derivative (structure **19**) showed similar or even higher bioactivity compared to the natural macrolide antibiotics (structures **2** and **5**). We also compared the bioactivity of structure **8** with its synthetic hydroxylated products. Unexpectedly, upon installation of a hydroxyl group at either the C7/C8 or C6/C9 positions (the four authentic standards, each of which contains a pair of diastereomers), the products lost activity. Although hydroxylation of structure **8** had a detrimental impact on biological activity against a limited number of microbial targets, installation of this functional group might enable a useful chemical handle for further functionalization (44) and subsequent generation of more potent therapeutics. Further analysis of these carbolides, and direct investigation of their presumed binding to ribosomal targets, will provide important insights into the impact of  $\text{PikC}$ -mediated regioselective hydroxylation for development of new small molecules for treatment of microbial pathogens and other human diseases.

## Conclusions

The work described in this article is based on the innate substrate flexibility of the biosynthetic P450  $\text{PikC}$  enzyme that could be harnessed using a substrate engineering strategy *in vitro* because of its desosamine-anchoring functionality. In contrast to previous chemical approaches that have exploited proximal directing influences or inherent differences in C–H bond strengths, our approach utilizes the interactions of an engineered bacterial P450 enzyme with aminosugar (desosamine)-linked substrates that otherwise lack all of the functionality of the native biosynthetic intermediates. This approach provides the unique opportunity to obtain high-resolution crystallographic insights into the nature of the substrate-catalyst interactions, which has generally not been available with biomimetic and organometallic systems that achieve catalytic oxidation of unactivated C–H bonds. Attachment of desosamine to a number of unnatural aglycones (especially cyclic aglycones) via an acetal linkage leads to productive enzyme binding and considerable regioselectivity in the hydroxylation reactions. However, the level of regio- and stereoselectivity observed for natural macrolide substrate YC-17 (structure **1**) and narbomycin (structure **4**) was not achieved, which infers synergistic contributions of both desosamine and macrolactone portions of these endogenous substrates. Insights gained from structural analysis in the present study suggest that selectivity could be improved by (i) rigidifying the substrate structure, (ii) limiting conformational freedom by optimizing the complementarity between substrate size and shape and the volume of the active site, and (iii) increasing structural complexity of compounds to improve the specificity of their binding.

Currently, further investigations, including the applicability of this approach in selective oxidation of complex compounds of medicinal significance, the development of alternative and more chemically accessible glycosides (as well as alternative molecular anchors), and the development of diverse linkage groups, are in

progress. Additionally, the observed selectivity could be potentially exploited for building libraries of compounds with hydroxyl group functional handles for further synthetic transformations. Moreover, the ability to obtain enzyme/substrate cocrystal structures offers unique mechanistic insights, as well as a means to engineer P450 enzymes that display greater regio- and stereoselectivity. This type of reagent engineering is particularly amenable to biological catalysts, and provides effective approaches to tailor the catalytic outcome toward a desired synthetic goal. Finally, these findings suggest that in addition to PikC, diverse natural product P450s can be further harnessed for a substrate engineering approach to selectively oxidize C–H bonds, and to facilitate further chemical diversification of both synthetic and natural product molecules of biological interest.

## Materials and Methods

**Preparation of PikC<sub>D50N</sub>-RhFRED.** Using previously prepared pET28b-pikC-RhFRED as a template (38), site-directed mutagenesis was performed by following the QuikChange (Stratagene) protocol. The primers for mutagenesis were: forward, 5'-CACCCCGAGGGGAATGAGGTGTGGCTGG-3'; reverse, 5'-CCAGCCACCTCATTCCCCTCGGGGGT-3'. Protein expression and purification of PikC<sub>D50N</sub>-RhFRED followed the procedure developed previously (38).

**PikC<sub>D50N</sub>-RhFRED Assay.** The standard assay contains 5  $\mu$ M PikC<sub>D50N</sub>-RhFRED, 0.5 mM substrate, 2.5 mM NADPH, 0.25 Unit of glucose-6-phosphate dehydrogenase, and 5 mM glucose-6-phosphate for NADPH regeneration in 100  $\mu$ L of reaction buffer (50 mM NaH<sub>2</sub>PO<sub>4</sub>, pH 7.3, 1 mM EDTA, 0.2 mM dithioerythritol, and 10% glycerol). The reaction was carried out at 30 °C for 3 h and terminated by extraction using 3  $\times$  200  $\mu$ L of CHCl<sub>3</sub>. The resulting organic extract was dried by N<sub>2</sub> and redissolved in 120  $\mu$ L of methanol. The subsequent LC-MS analysis was performed on a ThermoFinnigan LTQ linear ion-trap instrument (Department of Pharmacology, University of Michigan) equipped with electrospray source and Surveyor HPLC system by using an XBridge C18 3.5  $\mu$ m 150 mm reverse-phase HPLC column under the following conditions: mobile phase

(A = deionized water + 0.1% formic acid, B = acetonitrile + 0.1% formic acid), 20% B for 3 min, 20 to 100% B over 25 min, 100% B for 5 min, 100 to 20% B over 1 min, 20% B for 15 min; flow rate, 0.21 mL/min. The substrate binding assays were performed as previously described (38).

**Crystallization, Data Collection, and Structure Refinement.** Crystallization conditions for PikC<sub>D50N</sub> complexes with structures 6 and 8 were identified by using commercial high throughput screening kits available in deep-well format (Hampton Research), a nanoliter drop-setting Mosquito robot (TTP Lab Tech) operating with 96-well plates, and a hanging-drop crystallization protocol. Optimization of conditions was carried out manually in 24-well plates. The protein from the 1 mM stock was diluted to 0.2 mM by mixing with structure 6 or structure 8 dissolved at 2 mM in 10 mM Tris-HCl, pH 7.5. Crystals of PikC<sub>D50N</sub>-structure 6 complex were obtained from 15% PEG 4000, 0.1 M Tris-HCl, pH 7.5; 200 mM MgCl<sub>2</sub>. Crystals of the PikC<sub>D50N</sub>-structure 8 complex were obtained from 12% PEG 8000, 0.1 M sodium cacodylate, pH 6.5, and 200 mM Li<sub>2</sub>SO<sub>4</sub>. Before data collection, the crystals were cryo-protected by plunging them into a drop of reservoir solution supplemented with 20% glycerol. Diffraction data were collected at 100 to 110 K at beamline 8.3.1 (Advanced Light Source, Lawrence Berkeley National Laboratory). Data indexing, integration, and scaling were conducted using HKL2000 software suite. Crystal structures were determined by molecular replacement using the atomic coordinates of the PDB ID code 2CG6 as a search model (see Table S2 in *SI Appendix*).

For full experimental details of biochemistry/crystallography and synthetic chemistry, see the *SI Appendix*.

**ACKNOWLEDGMENTS.** We thank Mr. Yousong Ding, Dr. Liangcai Gu, and Dr. Kathleen Noon for assistance with LC-MS analysis, Dr. Patricia Cruz Lopez for assistance with NMR structural analysis, and Mr. Tom McQuade and Ms. Martha J. Larson in the Center for Chemical Genomics, University of Michigan for assistance with automatic antibacterial assays. We also thank the staff members of beamline 8.3.1, James Holton, George Meigs, and Jane Tanamachi, the Advanced Light Source at Lawrence Berkeley National Laboratory for assistance. This work was funded by National Institutes of Health Grants RO1 GM078553 (to D.H.S. and L.M.P.) and RO1 GM57014 (to J.M.). The Advanced Light Source is supported by the Director, Office of Science, Office of Basic Energy Sciences, of the U.S. Department of Energy under Contract No. DE-AC02-05CH11231.

- Ortiz de Montellano PR (1995) *Cytochrome P450: Structure, Mechanism, and Biochemistry*. 2nd Ed. (Plenum Press, New York).
- Guengerich FP (2001) Common and uncommon cytochrome P450 reactions related to metabolism and chemical toxicity. *Chem Res Toxicol* 14:611–650.
- Coon MJ (2005) Cytochrome P450: Nature's most versatile biological catalyst. *Ann Rev Pharmacol Toxicol* 45:1–25.
- Dick AR, Sanford MS (2006) Transition metal catalyzed oxidative functionalization of C–H bonds. *Tetrahedron* 62:2439–2463.
- Crabtree RH (2001) Alkane C–H activation and functionalization with homogeneous transition metal catalysts: A century of progress—A new millennium in prospect. *J Chem Soc, Dalton Trans* 2437–2450.
- Bergman RG (2007) Organometallic chemistry: C–H activation. *Nature* 446:391–393.
- Labinger JA, Bercaw JE (2002) Understanding and exploiting C–H bond activation. *Nature* 417:507–514.
- Godula K, Sames D (2006) C–H bond functionalization in complex organic synthesis. *Science* 312:67–72.
- Que L, Jr, Tolman W (2008) Biologically inspired oxidation catalysis. *Nature* 445:333–340.
- Chen MS, White CM (2007) A predictably selective aliphatic C–H oxidation reaction for complex molecule synthesis. *Science* 318:783–787.
- Brodsky BH, Du Bois J (2005) Oxaziridine-mediated catalytic hydroxylation of unactivated 3° C–H bonds using hydrogen peroxide. *J Am Chem Soc* 127:15391–15393.
- Wender PA, Hillinski MK, Mayweg AV (2005) Late-stage intermolecular CH activation for lead diversification: A highly chemoselective oxyfunctionalization of the C-9 position of potent bryostatins analogues. *Org Lett* 7:79–82.
- Lee S, Fuchs PL (2002) Chemospecific chromium(VI) catalyzed oxidation of C–H bonds at –40 °C. *J Am Chem Soc* 124:13978–13979.
- Chen H, Schlecht S, Semple TC, Hartwig JF (2000) Thermal, catalytic, regioselective functionalization of alkanes. *Science* 287:1995–1997.
- Cook BR, Reinert TJ, Suslick KS (1986) Shape-selective alkane hydroxylation by metalloporphyrin catalysts. *J Am Chem Soc* 108:7281–7286.
- Desai LV, Hull KL, Sanford MS (2004) Palladium-catalyzed oxygenation of unactivated sp<sup>3</sup> C–H bonds. *J Am Chem Soc* 126:9542–9543.
- Dick AR, Hull KL, Sanford MS (2004) A highly selective catalytic method for the oxidative functionalization of C–H bonds. *J Am Chem Soc* 126:2300–2301.
- Dangel BD, Johnson JA, Sames D (2001) Selective functionalization of amino acids in water: A synthetic method via catalytic C–H bond activation. *J Am Chem Soc* 123:8149–8150.
- Das S, Incarvito CD, Crabtree RH, Brudvig GW (2006) Molecular recognition in the selective oxygenation of saturated C–H bonds by a dimanganese catalyst. *Science* 312:1941–1943.
- Das S, Brudvig GW, Crabtree RH (2008) High turnover remote catalytic oxygenation of alkyl groups: How steric exclusion of unbound substrate contributes to high molecular recognition selectivity. *J Am Chem Soc* 130:1628–1637.
- Breslow R, et al. (1973) Remote oxidation of steroids by photolysis of attached benzophenone groups. *J Am Chem Soc* 95:3251–3262.
- Yang J, Gabriele B, Belvedere S, Huang Y, Breslow R (2002) Catalytic oxidations of steroid substrates by artificial cytochrome P-450 enzymes. *J Org Chem* 67:5057–5067.
- Grieco PA, Stuk TL (1990) Remote oxidation of unactivated carbon-hydrogen bonds in steroids via oxometalloporphyrins. *J Am Chem Soc* 112:7799–7801.
- Groves JT, Neumann R (1989) Regioselective oxidation catalysis in synthetic phospholipid vesicles. Membrane-spanning steroidal metalloporphyrins. *J Am Chem Soc* 111:2900–2909.
- Urlacher VB, Eiben S (2006) Cytochrome P450 monooxygenases: Perspectives for synthetic application. *Trends Biotechnol* 24:324–330.
- Landwehr M, Carbone M, Otey CR, Li Y, Arnold FH (2007) Diversification of catalytic function in a synthetic family of chimeric cytochrome P450s. *Chem Biol* 14:269–278.
- Sieber V, Martinez CA, Arnold FH (2001) Libraries of hybrid proteins from distantly related sequences. *Nat Biotechnol* 19:456–460.
- Arnold FH (2006) Fancy footwork in the sequence-space shuffle. *Nat Biotechnol* 24:328–330.
- Bloom JD, et al. (2005) Evolving strategies for enzyme engineering. *Curr Opin Struct Biol* 15:447–452.
- Kumar S, Chen CS, Waxman DJ, Halpert JR (2005) Directed evolution of mammalian cytochrome P450 2B1. *J Biol Chem* 280:19569–19575.
- Bloom JD, Arnold FH (2009) In the light of directed evolution: pathway of adaptive protein evolution. *Proc Natl Acad Sci USA* 106:9995–10000.
- Xue Y, Wilson D, Zhao L, Liu H-w, Sherman DH (1998) Hydroxylation of macrolactones YC-17 and narbomycin is mediated by the pikC-encoded cytochrome P450 in *Streptomyces venezuelae*. *Chem Biol* 5:661–667.
- Anzai Y, et al. (2008) Functional analysis of MycG and MycI, cytochrome P450 enzymes involved in biosynthesis of mycinamicin macrolide antibiotics. *Chem Biol* 15:950–959.
- Griengl H, de Raadt A (2002) The use of substrate engineering in biohydroxylation. *Curr Opin Biotechnol* 13:537–542.
- Lairson LL, Watts AG, Wakarchuk WW, Withers SG (2006) Using substrate engineering to harness enzymatic promiscuity and expand biological catalysis. *Nat Chem Biol* 2:724–728.
- Braunegg G, et al. (1999) The concept of docking/protecting groups in biohydroxylation. *Angew Chem Int Ed* 38:2763–2766.
- de Raadt A, Griengl H, Weber HJ (2001) The concept of docking and protecting groups in biohydroxylation. *Chem Eur J* 7:27–31.
- Li S, Podust LM, Sherman DH (2007) Engineering and analysis of a self-sufficient biosynthetic cytochrome P450 PikC fused to the RhFRED reductase domain. *J Am Chem Soc* 129:12940–12941.
- Xue Y, Zhao L, Liu H-w, Sherman DH (1998) A gene cluster for macrolide antibiotic biosynthesis in *Streptomyces venezuelae*: Architecture of metabolic diversity. *Proc Natl Acad Sci USA* 95:12111–12116.
- Sherman DH, et al. (2006) The structural basis for substrate anchoring, active site selectivity, and product formation by P450 PikC from *Streptomyces venezuelae*. *J Biol Chem* 281:26289–26297.
- Li S, Ouellet H, Sherman DH, Podust LM (2009) Analysis of transient and catalytic desamine-binding pockets in cytochrome P-450 PikC from *Streptomyces venezuelae*. *J Biol Chem* 284:5723–5730.
- Muralidhara BK, Halpert JR (2007) Thermodynamics of ligand binding to P450 2B4 and P450eryF studied by isothermal titration calorimetry. *Drug Metab Rev* 39:539–556.
- Schlünzen F, et al. (2001) Structural basis for the interaction of antibiotics with the peptidyl transferase centre in eubacteria. *Nature* 413:814–821.
- Rentmeister A, Arnold FH, Fasan R (2009) Chemo-enzymatic fluorination of unactivated organic compounds. *Nat Chem Biol* 5:26–28.